論文 84-21-3-12

Embedded Waveform Coding of Speech

(음성 파형의 Embedded 부호화에 관한 연구)

李 榮 豪*, 殷 鍾 官**

(Hyoung Ho Lee and Chong Kwan Un)

要 約

본 논문에서는 embedded ADPCM, embedded ADM 및 delayed decision 방식을 사용한 system이 실제 음성을 부호화할 때 그 성능을 연구하였다. Embedded ADPCM과 ADM 부호화기는 종래의 ADPCM과 ADM 부호화기를 개조함으로써 얻어졌다. Embedded ADPCM 부호화기는 기본적으로 Cummiskey 에 의해 최초로 제안된 바 있는 ADPCM을 기초로 하고 있다. Embedded ADM system은 CVSD와 HCDM system을 개조하여 만들었다. 이들 embedded 부호화기 중에서 embedded HCDM의 성능이 다른 부호화기에 비하여 16kbits/s에서 64kbits/s의 넓은 범위의 전송률에 걸쳐 우수하다. Embedded ADPCM에 delayed decision 방식을 적용하면 모든 전송률에서 성능이 크게 향상된다. 그러나 16kHz로 sample되는 embedded ADM system에 있어서는 같은 수의 지연 sample을 가진 embedded ADPCM에서 만큼 크게 성능이 향상되지는 않음을 알아내었다.

Abstract

The performances of embedded adaptive differential pulse code modulation (ADPCM), embedded adaptive delta modulation (ADM), and the same systems with a delayed-decision scheme have been studied with real speech over a wide dynamic range. The embedded ADPCM and ADM coders have been obtained by modifying the conventional ADPCM and ADM coders. The basic scheme of the embedded ADPCM coder is based on the ADPCM orginally proposed by Cummiskey et al. For embedded ADM systems, we have modified continuously variable slope DM (CVSD) and hybrid companding DM (HCDM) systems. Among these embedded coders, the performance of the embedded HCDM is superior to the other coders over a wide range of transmission rate from 16 to 64 kbits/s. When the delayed-decision scheme is applied to the embedded ADPCM the performance is improved significantly at all transmission rates. But, in the embedded ADM systems with 16 kHz sampling rate, the performance improvement resulting from delayed decision is not drastic as is in the embedded ADPCM with the same number of delayed samples.

*正會員, 韓國電氣通信研究所
(Korea Electrotechnology and Telecommunication Research Institute)

**正會員, 韓國科學技術院 電氣 및 電子工學科
(Dept. of Electrical Eng., KAIST)

接受日字 : 1984年 1月 18日

I. Introduction

A current research area of considerable interest in speech coding is variable rate coding. When variable rate coding is used in speech transmission, voice flow control can be made effectively by allowing the transmission bit rate

to change according to the variations of available channel bandwidth and traffic load. Typical areas of application of variable rate coding are speech interpolation systems, packet-switched systems, and integrated voice/data transmission systems.

In general, there are two approaches to varying the bit rate in transmission of speech. One approach is to control directly the speech encoder and decoder to operate at the bit rate set by the transmission system. The other approach is to control the bit rate within the transmission system without the interaction between the transmission system and the speech coder. Recently, several variable rate speech coders appropriate for the first approach have been proposed in wave form coding and vocoding[1]-[5]. Another type of variable rate coding technique is embedded coding, which is appropriate for the second approach in varying the bit rate. In packet transmission of speech by the embedded coding technique[6], a certain number of subpackets of successively lower priority are embedded in each packet being transmitted. Hence, the reception of any number of higher priority subpackets in a packet is sufficient for adequate decoding, although the reception of the entire packet gives the best quality. Speech transmission by some vocoding schemes fits naturally to the embedded coding concept. The residual-excited linear prediction (RELP) vocoder[7] can be considered as a two-rate embedded coder, since the system functions like a conventional low-rate linear prediction vocoder if the baseband residual is not received. As for waveform coding, pulse code modulation (PCM) coder may be considered as an embedded coder in that a PCM code word has a hierachy of bits of differing significance. However, conventional differential PCM (DPCM) by itself is not an embedded coder. Recently, a robust embedded DPCM structure has been developed by modifying the conventional DPCM structure[8].

In this paper, we introduce the embedded coding concept to the conventional adaptive differential coders such as adaptive DPCM (ADPCM) and adaptive delta modulation (ADM), and study their performances. Also, to improve the performance of embedded adaptive differential coders, we investigate the delayed-decision versions of those with a new decision criterion.

Following the introduction, we describe the embedded coder algorithms under study in Section II. Computer simulation results and discussion on system performance follow in Section III. Finally, we make conclusions in Section IV.

II. Embedded Adaptive Waveform Coding Algorithms

1. Embedded Adaptive Differential PCM

The structure of a general embedded adaptive differential PCM (EADPCM) coder is shown in Fig. 1. It consists of a conventional ADPCM coder for coding the difference signal r_n by B bits/sample and an additional coder for coding the quantized error signal $q_n=r_n-\hat{r}_n$ by R bits/sample. The transmission rate (or transmitted bits/sample) can be controlled from B to A(=B+R) bits/sample by bit stripping and inserting operation in the variable rate channel.

The ADPCM coder used in the EADPCM

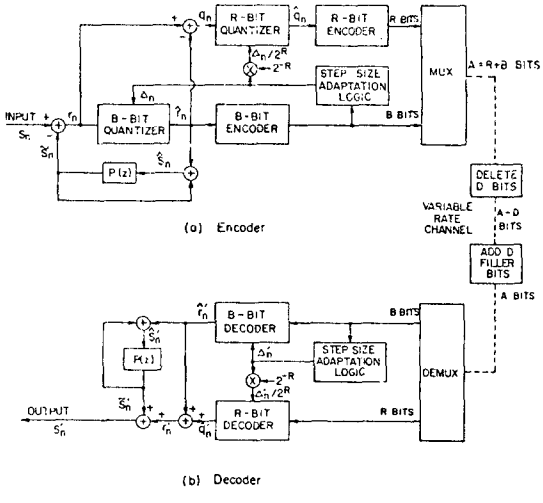

Fig. 1. Block diagram of EADPCM.

coder employs an adaptive quantization scheme with one-word memory developed by Cummiskey et al.[9]. The ADPCM coding structure is the same as that of the DPCM coding except for the use of a step-size adaptation logic. The step -size adaptation logic examines the B-bit quantizer output bits for the n-th sample and computes the quantizer step size Δ_{n+1} for the (n+1)-th sample according to the following rule:

$$\Delta_{n+1} = \Delta_n M(|H_n|), \tag{1}$$

and

$$\Delta_{min} \leq \Delta_{n+1} \leq \Delta_{max}, \tag{2}$$

where $M(|H_n|)$ is a multiplication factor whose value depends on the quantizer output level H_n at time n. For practical reasons, the step size Δ_n is constrained to be between some minimum and maximum values, Δ_{min} and Δ_{max}. With the mid-riser quantizer, optimal values of multiplier M_i for 2-, 3-, 4-, and 5-bit ADPCM coders are given in [9]. For the prediction filter in the feedback path of the ADPCM coder, we use a first-order fixed predictor given by

$$P(z) = a_1 z^{-1}, \tag{3}$$

where a_1 is a prediction coefficient.

For coding the quantizer error signal q_n we use an R-bit uniform mid-riser quantizer with the input-output relationship shown in Fig. 2(a). Its step size Δ_q at the time n is determined by the relation

$$\Delta_q = \Delta_n / 2^R, \tag{4}$$

where Δ_n is the step size of the B-bit quantizer at the time n. For embedded coding, the quantization-error signal coder uses a sign-magnitude binary format in representation of the error signal level. Fig. 2(a) shows 8-level quantization (R=3 bits) and 4-bit binary numbers which represent the odd multiples of $\Delta_q/2$ or quantized signal level. For 3-bit/sample transmission, the least significant bit (i.e., the fourth bit) that is always one is dropped and reinserted at the receiver. For 2-bit/sample transmssion with this representation, we drop the fourth and third bits of Fig. 2(a), and insert 1 for the third bit and 0 for the fourth bit at the receiver. This results in desirable quantization characteristic of Fig. 2(b), which has the same form as that of Fig. 2(a) except the reduction of the number of quantization levels and the increase of the step size by the same factor of 2.

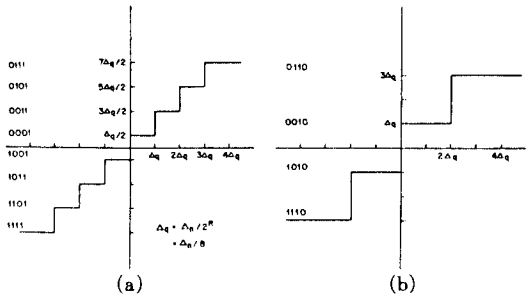

Fig. 2. Quantizer characteristics for coding quantization error signal.
(a) 3-bit mid-riser quantizer with step Δ_q.
(b) 2-bit mid-riser characteristic corresponding to (a).

In general, with the sign-magnitude representation of the mid-riser quantizer output, we can reduce the number of transmitted bits for a quantizer error signal sample from R to R-D by dropping D least significant bits. Then, at the receiver we append to the R-D received bits D+1 filler bits consisting of one 1 followed by D 0's. By doing so, we obtain a lower transmission bit rate at the expense of somewhat degraded quality of speech. In this case the original signal is reconstructed by a coarse decoder which has a larger step size and smaller number of reconstruction levels than those of the original R-bit decoder by the same factor of 2^D.

After multiplexing B-bits and R-bits information, total information bits (A=B+R) are sent to the variable rate channel where the

process of bit dropping and inserting is done. As seen in Fig. 1(b), the reconstructed signal s'_n is given by

$$\begin{aligned} s'_n &= \tilde{s}'_n + r'_n \\ &= \tilde{s}'_n + \hat{r}'_n + \hat{q}'_n \\ &= \hat{s}'_n + \hat{q}'_n \end{aligned} \tag{5}$$

From the above equation, we get $s'_n = \hat{s}'_n$ if $\hat{q}'_n = 0$. This means that the reconstructed value s'_n is equal to that of the conventional ADPCM coder if no information for the quantization error signal $\hat{q}'_n$ is additionally transmitted.

2. *Embedded Adaptive Delta Modulation (EADM)*

Delta modulation is a simple predictive coding method that is essentially equivalent to a 1-bit DPCM. Hence, we can apply the embedded coding technique to a conventional ADM as done for ADPCM. Among many different DM algorithms, those selected for the embedded DM coding study are continuously variable slope delta modulation (CVSD)[10] and hybrid companding DM (HCDM)[11]. Detailed description of these systems and their performances at 16 and 24 kbits/s are discussed in [10]. In this section, our discussion will focus only on important features of each EADM coder algorithm including the embedded structure.

1) Embedded Continuously Variable Slope DM(ECVSD)

A block diagram of ECVSD is shown in Fig. 3. It consists of a conventional CVSD encoder coding 1 bit/sample and a residual encoder coding R bits/sample. In a CVSD coder the quantizer step size Δ_n is controlled by a syllabic compandor which consists of a 3-bit shift register, a comparator, and a syllabic filter with a syllabic time constant $1/\alpha$. The step size adaptation rule is as follows:

$$\begin{aligned} \Delta_n &= e^{-\alpha T}\Delta_{n-1} + \Delta_{max}(1-e^{-\alpha T}), \\ &\quad \text{if } b_n = b_{n-1} = b_{n-2}, \\ &= e^{-\alpha T}\Delta_{n-1}, \text{ otherwise,} \end{aligned} \tag{6}$$

and

$$\Delta_{min} \le \Delta_n \le \Delta_{max}, \tag{7}$$

where T is a sampling interval, and Δ_{min} and Δ_{max} are minimum and maximum step sizes, respectively. The prediction of input signal s_n is performed by a leaky integrator with a prediction time constant $1/\beta$. Hence, the reconstructed signal $\hat{s}_n$ is given by

$$\hat{s}_n = e^{-\beta T}\tilde{s}_{n-1} + b_{n-1}\Delta_{n-1}, \tag{8}$$

where $\tilde{s}_n$ is the predicted value of s_n.

Now, we obtain the residual signal q_n by subtracting $\hat{s}_n$ from s_n. This residual error signal is quantized and encoded in the same manner as in the EADPCM discussed before. Note that from (8), the DM quantizer with an ideal integrator is equivalent to the one-bit mid-riser quantizer with the step size of $2\Delta_n$. Hence, the step size of the R-bit mid-riser residual quantizer is determined by

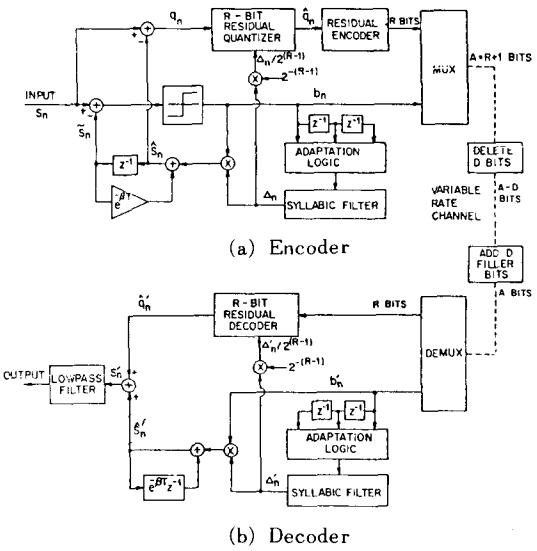

Fig. 3. Block diagram of ECVSD.

$$\Delta_q = 2\Delta_n/2^R = \Delta_n/2^{(R-1)}. \quad (9)$$

Of course, the residual quantizer operates at the same sampling rate as the DM encoder.

2) Embedded Hybrid Companding DM (EHCDM)

The embedded ADM coder with hybrid companding is shown in Fig. 4. The residual quantization and encoding methods are the same as those of the ECVSD described above. The HCDM encoder used in EHCDM is the same as the conventional HCDM encoding system [11]. This system employs both syllabic and instantaneous companding schemes in varying the quantizer step size. The former is used to update the long term basic step size Δ_H of the quantizer according to the slope energy of the decoded signal that is estimated every 5 ms. The later is used for changing the step size at every sampling instant. Hence, given an input sample s_n, the output b_n is generated as

$$b_n = \mathrm{sgn}(s_n - \tilde{s}_n)$$

with

$$\tilde{s}_n = e^{-\beta T}\tilde{s}_{n-1} + b_{n-1}\Delta_{n-1}, \quad (10)$$

$$\Delta_n = \gamma_n \Delta_H,$$

$$\gamma_n = k_n \gamma_{n-1},$$

and

$$k_n = f(b_n, b_{n-1}, b_{n-2}),$$

where k_n is a multiplication factor that depends on the present and two previous bits and is determined by a logic rule tabulated in [11]. The basic step size Δ_H is obtained by

$$\Delta_H = \alpha_H E,$$

and (11)

$$E = \sqrt{\sum_{i=1}^{J-1} \frac{(\tilde{s}_i - \tilde{s}_{i-1})^2}{J-1}},$$

where Δ_H is a constant less than one, and J is the number of input samples in 5 ms.

3. Embedded Adaptive Waveform Coders with Delayed Decision

Subjective or objective quality of speech depends on two different types of distortion; granular noise and slope overload noise. Granular noise is caused by the quantizer having only a finite number of levels in representation of the input signal. On the other hand, overload noise occurs when the input signal increases to a level that is larger than the system can encode. For a B-bit uniform mid-riser quantizer with the step size Δ_n, the overload noise occurs when the input signal amplitude exceeds $2^{B-1}\Delta_n$. Below this level, granular noise occurs. When overload occurs, quantization noise is dominated by overload distortion. Otherwise, granular noise is the only source of distortion. In conventional embedded waveform coders discussed above, the amount of granular noise caused by the quantizer can be reduced by additional encoding of error signal, but overload noise caused by the quantizer cannot be reduced because of the limitation of the quantizer range of the second coder. Hence, the performance of an embedded waveform coder at a high transmission rate is greatly affected by the amount of overload noise generated by the quantizer. This is a disadvantage of conventional embedded waveform coding. To alleviate this problem, we investigate an embedded waveform coder with delayed desicion. It is well known that a waveform coding system with a delayed-decision scheme results in improved SQNR and dynamic range over the system without it[12]-[14]. This improvement of SQNR is mainly due to a large amount of reduction in overload noise. Hence, if we adopt this feature of the delayed-decision scheme in a conventional embedded waveform coder, the performance of the embedded coder can be effectively improved, particularly at higher transmission rates.

A block diagram of a delayed-decision coder is shown in Fig. 5. In this system, for delayed-decision operation before final encoding, the encoder has a buffer, a tree generator, and a searching algorithm, while the decoder has the

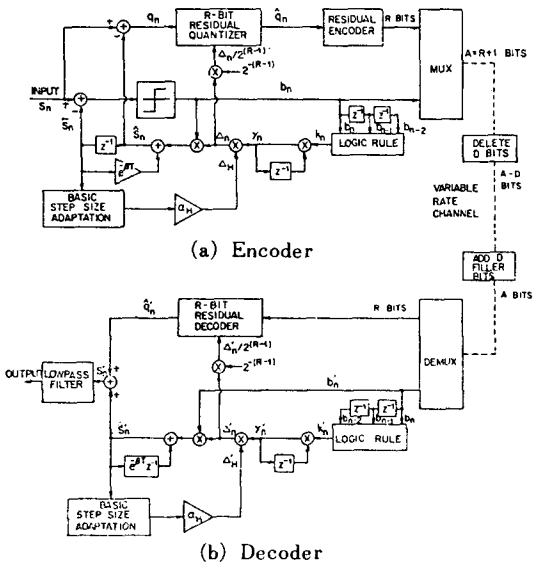

Fig. 4. Block diagram of EHCDM.

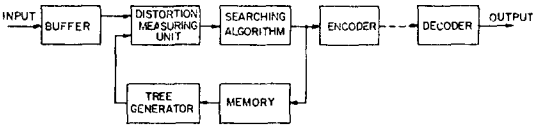

Fig. 5. Block diagram of delayed-decision coder.

same structure as that of the conventional coder. As shown in Fig. 5, a sequence of N_b speech samples, $X=[x_1, x_2, \ldots, {}^{x}N_b]$, is stored in a buffer, and then a tree generator generates a sequence of N_b sample codes that are equivalent to the quantizer output levels of the conventional coder. By using a predefined distortion measure, the searching algorithm finds the most suitable sequence among $2^{B\cdot N_b}$ possible sequences when a B-bit quantizer is used. That is, the searching algorithm compares the input $\bar{X}$ with a collection of possible output sequences $\bar{Y}_n$, n=1,2,3, . . . , $2^{B\cdot N_b}$ where $\bar{Y}_n^T=[y_{n1}, y_{n2}, \ldots, y_{nN_b}]$, and chooses the optimum output sequence with the smallest squared error

$$E_n=(\bar{X}-\bar{Y}_n)^T.(\bar{X}-\bar{Y}_n). \tag{12}$$

The encoder chooses the output sequence that gives the smallest E_n, and outputs the corresponding binary code sequence or at least a portion of it according to the decision rule. At the same time, the values such as step size and predicted value that are necessary for the next decision must be stored in the memory. In sample-by-sample decision, the same decision procedure is repeated every sampling interval for transmission of the first output sample in the chosen output sequence consisting of N_b output samples.

1) EADPCM with Delayed Decision (EADPCM-DD)

Let us consider a new delayed-decision algorithm which is suitable for EADPCM shown in Fig. 1. When all B and R bits for quantization error signal q_n are transmitted without channel errors, the reconstructed signal s_n' in the decoder is represented by

$$\begin{aligned} s_n' &= \hat{s}_n' + \hat{q}_n' \\ &= \hat{s}_n + \hat{q}_n, \end{aligned} \tag{13}$$

where $\hat{q}_n$ is the quantized value of q_n. Also, q_n, $\hat{s}_n$, and $\tilde{s}_n$ are given as follows:

$$q_n = r_n - \hat{r}_n, \tag{14}$$

$$\hat{s}_n = \tilde{s}_n + \hat{r}_n, \tag{15}$$

$$\tilde{s}_n = s_n - r_n. \tag{16}$$

Combining (14), (15), and (16), we have

$$\hat{s}_n = s_n - r_n + \hat{r}_n = s_n - q_n. \tag{17}$$

Inserting (17) in (13), we have

$$s_n' = s_n - q_n + \hat{q}_n = s_n - (q_n - \hat{q}_n). \tag{18}$$

Here, we define the distortion measure as the squared error signal given by

$$E_n = \sum_{k=n}^{n+K_d} (s_k - s_k')^2 = \sum_{k=n}^{n+K_d} (q_k - \hat{q}_k)^2, \tag{19}$$

where K_d is the number of delayed speech samples. By using the above distortion measure, the EADPCM-DD encoder takes the role of reducing the quantization error of the R-bit quantizer $q_n - \hat{q}_n$ in (18) as small as possible for accurate coding of speech signal.

2) Embedded ADM's with Delayed Decision

We can apply the delayed-decision scheme shown in Fig. 5 to the two embedded ADM's shown in Figs. 3 and 4. When all R bits for the residual signal q_n and an ADM output bit are transmitted without channel error, the reconstructed signal s_n' in the decoder and the distortion measure E_n can be written by (18) and (19), respectively. Using the distortion measure, the embedded ADM coder with a delayed-decision scheme decides one output code (R bits for residual quantization and 1 bit for ADM output) in every sampling interval.

III. Computer Simulation Results and Discussion

Simulation of the embedded waveform coders has been done on a mini-computer with real speech signals bandlimited to 3.4 kHz and sampled at 8 and 16 kHz. Speech samples used for simulations have been made from five sentences spoken by three male and two female speakers. The total length of the speech samples is about 15 s long. We have used an 8-pole Butterworth low-pass filter (LPF) to bandlimit the input and decoded signals. The configuration used in this simulation study is shown in Fig. 6. To simulate efficiently the embedded coding algorithms at (R+1) different transmission rates, we have used (R+1) identical decoders and low-pass filters at the receiver. After encoding a speech sample with A bits (R bits for coding quantizer error signal and B bits for coding prediction error), the number of transmitted bits is changed sequentially from A bits to B bits by bit deleting and inserting operations. At the same time, the received binary data is passed to one of the (R+1) decoders according to the number of transmitted bits. This procedure generates simultaneously (R+1) decoded signals which are used for the measurement of objective performance of the embedded coder at (R+1) different transmission rates.

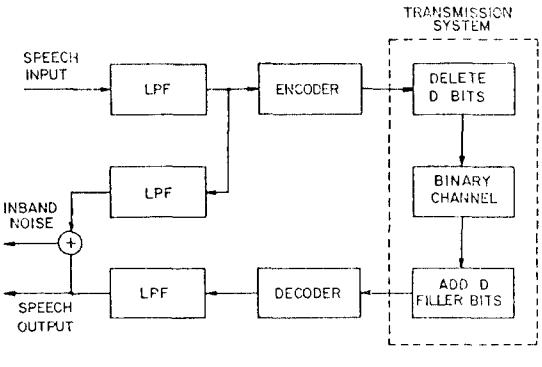

Fig. 6. Block diagram of the simulation procedure.

To measure the performance of an embedded coder, we have used the segmented SQNR($SQNR_{SEG}$) defined as

$$SQNR_{SEG} = \frac{1}{I}\sum_{i=0}^{I-1} 10 \log\left(1+\frac{\sum_{n=1}^{J} s^2_{n+iJ}}{\sum_{n=1}^{J} (s_{n+iJ}-\hat{s}_{n+iJ})^2}\right), \quad (20)$$

where s_n is the n-th input sample of the input speech and $\hat{s}_n$ is its reproduction. The number of total speech samples is I·J where I is the total number of frames, each composed of J speech samples. In this simulation study, one frame length of speech has been chosen to be 20ms long (i.e., J is equal to 160 when the sampling rate is 8 kHz and 320 when the rate is 16 kHz).

The waveform coders under study have been simulated with a step size range of 60 dB. Prior to getting performance measures, the coefficient of the first-order fixed predictor for ADPCM and the time constants of the syllabic and prediction filters for ADM's were optimized so that maximum SQNR may be obtained. The ADPCM prediction

coefficient was set to 0.91. And the ADM syllabic and prediction time constants were set to 5 and 1.6 ms at the 16 kHz sampling rate, respectively. We have used the same parameter values for the two ADM systems, since the variation of these values resulted in a negligible improvement of performance in each coder.

With the parameter values optimized, we have obtained the plots of $SQNR_{SEG}$ as a function of transmission rate and input signal level. For practical reasons, we limited the encoding bit rate (or the maximum transmission rate) to 64 kbits/s.

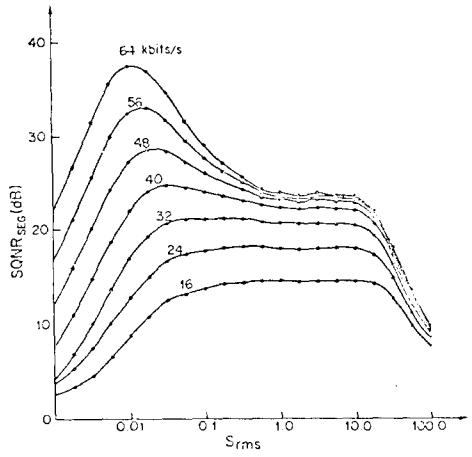

Fig. 7. $SQNR_{SEG}$ of EADPCM2 with different transmission rates vs. input signal level.

In simulation of the EADPCM system, we have obtained the performances of the system with 2-, 3-, and 4-bit ADPCM quantizers. Fig. 7 shows the performance of the EADPCM system with 2-bit ADPCM quantizer (EADPCM2). From this figure, we can see that peak SQNR occurs at a low signal level regardless of transmission rate. Also, as the transmission rate increases, the maximum SQNR becomes peakier and shifts towards the lower signal level. This phenomenon can be explained as follows. In a higher range of input signal level, the step size of the adaptive quantizer is limited to the maximum step size Δ_{max}. Hence, the quantization noise is dominated by slope overload distortion, which cannot be reduced by the additional coder for the quantization error signal in a conventional embedded coder. In the middle range of input signal level, the ADPCM coder has both granular and slope overload noise to track the input signal variation. In this region, the performance of the embedded coder at a high transmission rate depends largely on the slope overload noise, since only the granular noise can be reduced by additional encoding of quantization error. From the simulation results we can see that, as the transmission rate increases, $SQNR_{SEG}$ increases slowly and levels off at a high transmission rate. This means that the amount of slope overload noise is comparable to that of granular noise in the middle range of input signal level. As the input signal level decreases, the central step size of the adaptive quantizer also decreases since it adapts to the input signal variation. At a lower signal level, the variation of the quantizer step is limited to the minimum step size Δ_{min}. Hence, as the input signal decreases, the ratio of granular noise caused by quantization to input signal increases slowly. On the other hand, the ratio of slope overload noise to input signal decreases fast. Accordingly, SQNR increases fast and reaches to the value of peak SQNR at a certain signal level, at which the granular noise is much larger than slope overload noise. As the signal level decreases further, the slope overload noise no longer exists, only the granular noise remaining. This granular noise can be reduced by additional coding. As seen in the simulation results, the amount of increase in SQNR for each one-bit increase in bit per sample is almost the same (about 5 dB/bit/sample).

Fig. 8 shows the $SQNR_{SEG}$ performances of EADPCM system with 4-bit quantizer (EADPCM4). Here, it is worthwhile to note that $SQNR_{SEG}$ at the same transmission rate is increased as the number of bits of the ADPCM quantizer increases. Of course, as the number of quantizer levels is increased, the

minimum transmission rate is also increased. From Figs. 7 and 8, we can conclude that compared with the conventional ADPCM, EADPCM yields far inferior performance at high transmission rates.

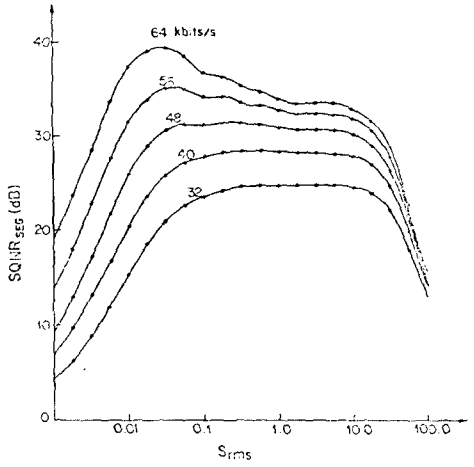

Fig. 8. SQNR$_{SEG}$ of EADPCM4 with different transmission rates vs. input signal level.

In order to improve the performance of EADPCM, we have studied the EADPCM coder with a delayed-decision scheme(EADPCM -DD). The decision criterion chosen for the

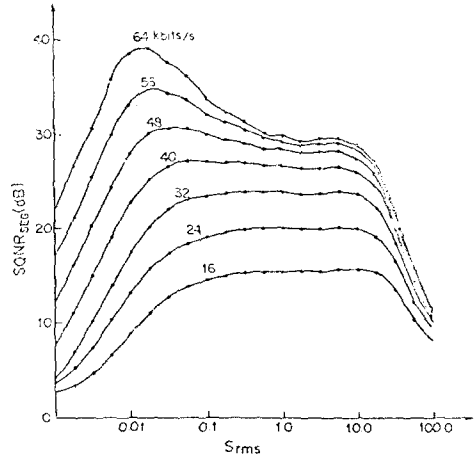

Fig. 9. SQNR$_{SEG}$ of EADPCM2-DD1 with different transmission rates vs. input signal level.

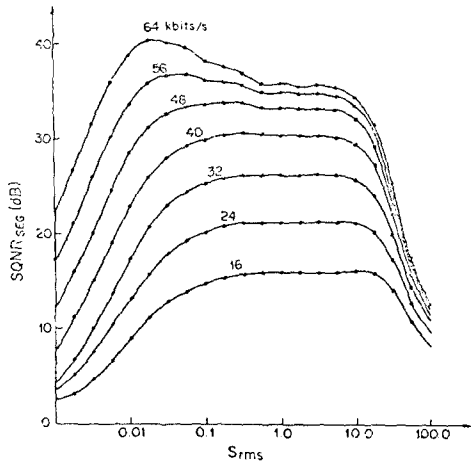

Fig.10. SQNR$_{SEG}$ of EADPCM2-DD3 with different transmission rates vs. input signal level.

EADPCM-DD has been discussed in Section II. Figs. 9 and 10 show the SQNR SEG performance of EADPCM2 with one- and three-sample delay (EADPCM2-DD1 and -DD3), respectively. Of course, as the number of delayed samples increases, the performance of EADPCM is significantly improved, particularly at higher transmission rates. Hence, the overall performance of EADPCM2-DD1 is nearly the same as that of EADPCM4. In EADPCM2-DD3 all the performance curves are nearly flattened over a wide range of input signal level.

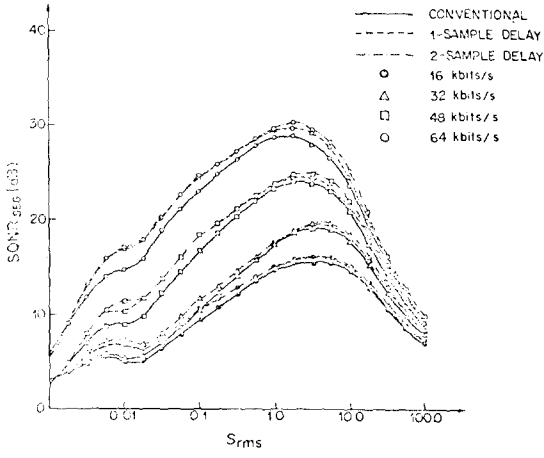

Fig.11. SQNR$_{SEG}$ of ECVSD systems with different transmission rates vs. input signal level.

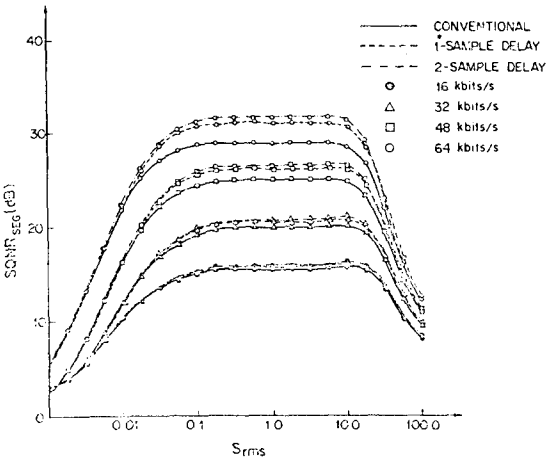

Fig.12. $SQNR_{SEG}$ of EHCDM systems with different transmission rates vs. input signal level.

Finally, we have investigated the performance of embedded ADM coders with and without the delayed-decision scheme at the sampling rate of 16 kHz. Figs. 11 and 12 the $SQNR_{SEG}$ performances of ECVSD and EHCDM, each with and without delayed decision. These figures show that the performance improvement of EADM's resulting from the use of a delayed-decision scheme is not so drastic as compared with that of EADPCM-DD with the same number of sample delay. The performance of EADM systems at 16 kHz is comparable to that of EADPCM with a 2-bit ADPCM quantizer. Although EADPCM2 system has a larger peak $SQNR_{SEG}$ (or SQNR) value than that of EADM systems, EADM's retain better performance over a wide range of input signal level and transmission rate. Of those, EHCDM yields the best performance in $SQNR_{SEG}$ (or SQNR).

IV. Conclusions

We have studied the performances of EADPCM, EADM systems and the same systems with a delayed-decision scheme by computer simulation with real speech. The EADPCM system yields performance curves with narrow dynamic range at the middle range of input signal level, in which its $SQNR_{SEG}$ values at higher transmission rates are significantly lower than those of the conventional ADPCM with the same bit rates. But, the proposed EADPCM system with delayed decision tends to widen the dynamic range in its performance curves. In EADPCM-DD3, the performance curves are nearly flattened over a wide range of input signal level and transmission rate. Of course, when a delayed-decision is used, the performances of EADPCM are significantly improved. For each transmission rate, the proposed EADM coders have performance curves of which shapes are similar to those of the corresponding ADM coders. When the delayed decision is applied to EADM, the performance improvement in EADM systems at 16 kHz sampling rate is not so drastic as is in EADPCM systems with the same number of delayed samples.

Acknowledgement

The authors wish to thank the anonymous reviewer for his thorough review of the manuscript.

References

[1] J.J. Dubnowski and R.E. Crochiere, "Variable rate coding of speech," *Bell Syst. Tech. J.*, vol. 58, pp.577-600, Mar. 1979.

[2] R.V. Cox and R.E. Crochiere, "Multiple user variable rate coding for TASI and packet transmission systems," *IEEE Trans. Commun.*, vol. COM-28, pp.334-344, Mar. 1980.

[3] C.K. Un and D.H. Cho, "Hybrid companding delta modulation with variable-rate sampling," *IEEE Trans. Commun.*, vol. COM-30, pp.593-599, Apr. 1982.

[4] B.S. Lee et al., "Implementation of a multirate speech digitizer," *IEEE Trans. Commun.*, vol. COM-31, pp.775-783, June 1983.

[5] G. Rebolledo et al., "A multirate voice

digitizer based upon vector quantization," *IEEE Trans. Commun.*, vol. COM-30, pp.721-727, Apr. 1982.

[6] T. Bially et al., "A technique for adaptive voice flow control in integrated packet networks," *IEEE Trans. Commun.*, vol. COM-28, pp.325-333, Mar. 1980.

[7] C.K. Un and D.T. Magill, "The residual-excited linear prediction vocoder with transmission rate below 9.6kbits/s," *IEEE Trans. Commun.*, vol. COM-23, pp.1466-1474, Dec. 1975.

[8] D.J. Goodman, "Embedded DPCM for variable bit rate transmission," *IEEE Trans. Commun.*, vol. COM-28, pp.1040-1046, July 1980.

[9] P. Cummiskey et al. "Adaptive quantization in differential PCM coding of speech," *Bell Syst. Tech. J.*, vol. 52, pp.1105-1108, Sep. 1973.

[10] C.K. Un and H.S. Lee, "A study of the comparative performance of adaptive delta modulation systems," *IEEE Trans. Commun.*, vol. COM-28, pp.96-101, Jan. 1980.

[11] C.K. Un et al., "Hybrid companding delta modulation," *IEEE Trans. Commun.*, vol. COM-29, pp.1337-1344, Sep. 1981.

[12] J.B. Anderson and J.B. Bodie, "Tree encoding of speech," *IEEE Trans. Information Theory*, vol. IT-21, no. 4, pp.379-387, July 1975.

[13] N.S. Jayant and S.A. Christensen, "Tree-encoding of speech using the (M,L)-algorithm and adaptive quantization," *IEEE Trans. Commun.*, vol. COM-26, no. 9, pp.1376-1379, Sep. 1978.

[14] L.H. Zetterberg and J. Uddenfeldt, "Adaptive delta modulation with delayed decision," *IEEE Trans. Commun.*, vol. COM-22, pp.1195-1198, Sep. 1974